THE EUROPEAN PHYSICAL JOURNAL C

Pion freeze-out time in $Pb+Pb$ collisions at $158\,A\mathrm{GeV}/c$ studied via π^-/π^+ and K^-/K^+ ratios

The WA98 Collaboration

M.M. Aggarwal[1], Z. Ahammed[2], A.L.S. Angelis[3,†], V. Antonenko[4], V. Arefiev[5], V. Astakhov[5], V. Avdeitchikov[5], T.C. Awes[6,a], P.V.K.S. Baba[7], S.K. Badyal[7], S. Bathe[8], B. Batiounia[5], T. Bernier[9], K.B. Bhalla[10], V.S. Bhatia[1], C. Blume[8], D. Bucher[8], H. Büsching[8], L. Carlen[11], S. Chattopadhyay[2], M.P. Decowski[12], H. Delagrange[9], P. Donni[3], M.R. Dutta Majumdar[2], K. El Chenawi[11], A.K. Dubey[13], K. Enosawa[14], S. Fokin[4], V. Frolov[5], M.S. Ganti[2], S. Garpman[11,†], O. Gavrishchuk[5], F.J.M. Geurts[15], T.K. Ghosh[16], R. Glasow[8], B. Guskov[5], H. Å.Gustafsson[11], H.H. Gutbrod[17], I. Hrivnacova[18], M. Ippolitov[4], H. Kalechofsky[3], R. Kamermans[15], K. Karadjev[4], K. Karpio[19], B.W. Kolb[17], I. Kosarev[5,†], I. Koutcheryaev[4], A. Kugler[18], P. Kulinich[12], M. Kurata[14], A. Lebedev[4], H. Löhner[16], L. Luquin[9], D.P. Mahapatra[13], V. Manko[4], M. Martin[3], G. Martínez[9], A. Maximov[5], Y. Miake[14], G.C. Mishra[13], B. Mohanty[13], M.-J. Mora[9], D. Morrison[20], T. Mukhanova[4], D.S. Mukhopadhyay[2], H. Naef[3], B.K. Nandi[13], S.K. Nayak[9], T.K. Nayak[2], A. Nianine[4], V. Nikitine[5], S. Nikolaev[4], P. Nilsson[11], S. Nishimura[14], P. Nomokonov[5], J. Nystrand[11], A. Oskarsson[11], I. Otterlund[11], S. Pavliouk[5], T. Peitzmann[15], D. Peressounko[4], V. Petracek[18], S.C. Phatak[13], W. Pinganaud[9], F. Plasil[6], M.L. Purschke[17], J. Rak[18], R. Raniwala[10], S. Raniwala[10], N.K. Rao[7], F. Retiere[9], K. Reygers[8], G. Roland[12], L. Rosselet[3], I. Roufanov[5], C. Roy[9], J.M. Rubio[3], S.S. Sambyal[7], R. Santo[8], S. Sato[14], H. Schlagheck[8], H.-R. Schmidt[17], Y. Schutz[9], G. Shabratova[5], T.H. Shah[7], I. Sibiriak[4], T. Siemiarczuk[19], D. Silvermyr[11], B.C. Sinha[2], N. Slavine[5], K. Söderström[11], G. Sood[1], S.P. Sørensen[20], P. Stankus[6], G. Stefanek[19], P. Steinberg[12], E. Stenlund[11], M. Sumbera[18], T. Svensson[11], A. Tsvetkov[4], L. Tykarski[19], E.C. v. d. Pijll[15], N. v. Eijndhoven[15], G.J. v. Nieuwenhuizen[12], A. Vinogradov[4], Y.P. Viyogi[2], A. Vodopianov[5], S. Vörös[3], B. Wysłouch[12], G.R. Young[6]

1 University of Panjab, Chandigarh 160014, India
2 Variable Energy Cyclotron Centre, Calcutta 700064, India
3 University of Geneva, 1211 Geneva 4, Switzerland
4 RRC Kurchatov Institute, 123182 Moscow, Russia
5 Joint Institute for Nuclear Research, 141980 Dubna, Russia
6 Oak Ridge National Laboratory, Oak Ridge, Tennessee 37831-6372, USA
7 University of Jammu, Jammu 180001, India
8 University of Münster, 48149 Münster, Germany
9 SUBATECH, Ecole des Mines, Nantes, France
10 University of Rajasthan, Jaipur 302004, Rajasthan, India
11 Lund University, 22100 Lund, Sweden
12 MIT, Cambridge, MA 02139, USA
13 Institute of Physics, 751-005 Bhubaneswar, India
14 University of Tsukuba, Ibaraki 305, Japan
15 Universiteit Utrecht/NIKHEF, 3508 TA Utrecht, The Netherlands
16 KVI, University of Groningen, 9747 AA Groningen, The Netherlands
17 Gesellschaft für Schwerionenforschung (GSI), 64220 Darmstadt, Germany
18 Nuclear Physics Institute, 250 68 Rez, Czech Republic
19 Institute for Nuclear Studies, 00-681 Warsaw, Poland
20 University of Tennessee, Knoxville, Tennessee 37966, USA

† deceased

Abstract. The effect of the final state Coulomb interaction on particles produced in Pb + Pb collisions at $158\,A\text{GeV}/c$ has been investigated in the WA98 experiment through the study of the π^-/π^+ and K^-/K^+ ratios measured as a function of $m_\text{T} - m_0$. While the ratio for kaons shows no significant m_T dependence, the π^-/π^+ ratio is enhanced at small $m_\text{T} - m_0$ values with an enhancement that increases with centrality. A silicon pad detector located near the target is used to estimate the contribution of hyperon decays to the π^-/π^+ ratio. The comparison of results with predictions of the RQMD model in which the Coulomb interaction has been incorporated allows to place constraints on the time of the pion freeze-out.

1 Introduction

The distributions of negatively and positively charged pions produced in heavy ion collisions exhibit significant differences at low transverse kinetic energy (or transverse mass), $m_\text{T} - m_\pi = \sqrt{p_\text{T}^2 + m_\pi^2} - m_\pi$. These differences are evident in the behaviour of the ratio of their yields $R_\pi = \pi^-/\pi^+$. The study of charged particle production in Au + Au collisions at SIS ($1\,A\text{GeV}$) [1] and AGS ($10.8\,A\text{GeV}$) [2–4] shows that for central collisions R_π rises at low m_T at both collision energies. At the same time, for peripheral collisions at the AGS, R_π does not depend on m_T. At $1\,A\text{GeV}$ R_π is about 2.9 for $m_\text{T} - m_\pi$ near zero and its integrated value is $R_\pi = 1.9 \pm 0.1$. The large integrated value at $1\,A\text{GeV}$ can be explained by isobar decays and reflects the N/Z asymmetry of the colliding system. The very sharp rise at low m_T on the other hand points toward significant Coulomb interactions between charged pions and the remaining nuclear charge distribution (acceleration of π^+ and deceleration of π^-). At $10.8\,A\text{GeV}$ and higher energy the isobar contribution to R_π becomes insignificant and it is expected that mainly the Coulomb interaction distorts the R_π ratio. The NA44 experiment has published data on R_π measured in central Pb + Pb collisions at $158\,A\text{GeV}$ [5]. A prominent enhancement of R_π at small m_T was observed. NA44 has also measured R_π in S + S and S + Pb collisions at $200\,A\text{GeV}/c$, where the ratio remains constant at $m_\text{T} - m_\pi < 0.5\,\text{GeV}/c^2$ [5]. At high energies (AGS and SPS) the contribution from strange particle decay can significantly affect the measured pion distribution. The hyperon contribution is influenced by the detector acceptance and the pion vertex reconstruction properties. The excess of hyperon over anti-hyperon yield in heavy ion collisions also leads to an enhancement of R_π at low transverse kinetic energy.

Several dedicated models [6–11] describe the pion ratio detected by the NA44 collaboration in Pb + Pb collisions through the electromagnetic interaction induced by the large amount of charge of the participating protons. The authors of the dynamical model of [6] argue that the R_π enhancement at small momenta depends mainly on the time of freeze-out and extract a freeze-out time of about $7\,\text{fm}/c$. They also predict the corresponding ratio for kaons, $R_K = K^-/K^+$, to be smaller by a factor of m_K/m_π. However, this overestimates the NA44 kaon measurement. This discrepancy is explained as due to the much larger absorption of K^- on nucleons ($K^- + N \to \Lambda + \pi$) than for K^+. For a detector located at mid-rapidity this model predicts a small reduction of the R_π enhancement with respect to the NA44 result measured near rapidity $y_\text{CMS} = 1$ in the center of mass system. On the other hand, in another model [11] the enhancement of the ratio strongly increases towards mid-rapidity, reaching the value of 2.5. In [9] it is concluded that the influence of the Coulomb force should be computed within an event simulator which takes into account a more accurate description of the space-time evolution of the collision.

Initial results from the SPS experiment WA98 on the measurement of the π^-/π^+ ratio in central Pb + Pb collisions were reported in [12]. The enhancement of R_π at $m_\text{T} - m_\pi < 50\,\text{MeV}/c^2$ measured with the two independent tracking arms of WA98 located nearer to mid-rapidity than the NA44 spectrometer was reported to be significantly smaller than that measured by NA44 [5].

In this paper we present the π^-/π^+ ratio as a function of centrality for $158\,A\text{GeV}/c$ Pb + Pb collisions. The background pion contribution from hyperon decays is determined and removed by use of vertex information from a silicon detector located near to the target to obtain the ratio of pions that originate in the target. The yields of electrons and positrons are analysed at low momentum where they can be clearly identified through time-of-flight. Their yields provide a check of the normalization of the opposite sign yields at the lowest transverse momenta. They also confirm the validity of estimates of the electron and positron contaminations to the measured pion distributions at higher momenta. The K^-/K^+ ratio is also presented for central collisions. The results are compared with predictions of the RQMD 2.4 model [13] in which final state Coulomb interactions have been added. Within the uncertainties of the hyperon decay contribution the results are found to be compatible with predictions of the RQMD model in which the average pion freeze-out time is $15\,\text{fm}/c$ for central collisions. Possible modifications of the final state predicted by RQMD, necessary to improve agreement with the measured π^-/π^+ ratios, are investigated and discussed.

2 Experimental setup and data analysis

The CERN SPS experiment WA98 [14] combined photon and hadron spectrometers with other large acceptance detectors that measured a number of global variables on an event-by-event basis. Figure 1 shows the experimental layout during the $158\,A\text{GeV}$ ^{208}Pb beam run period in 1996 with a $0.239\,\text{g}/\text{cm}^2$ Pb target.

The Mid-Rapidity Calorimeter, MIRAC [15], measured the collision transverse energy (E_T) in the pseudorapidity
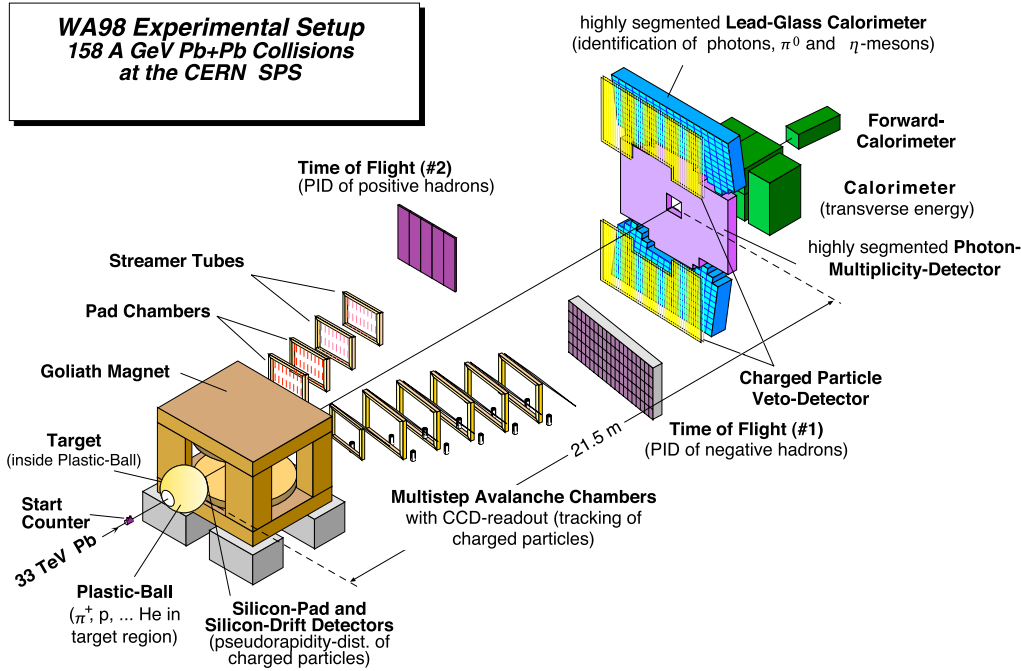
$^\text{a}$ awes@mail.phy.ornl.gov

WA98 Experimental Setup
*158 A GeV Pb+Pb Collisions
at the CERN SPS*

highly segmented **Lead-Glass Calorimeter**
(identification of photons, π^0 and η-mesons)

Fig. 1. The WA98 experimental setup

Time of Flight (#2)
(PID of positive hadrons)

Forward-Calorimeter

Calorimeter
(transverse energy)

highly segmented **Photon-Multiplicity-Detector**

Streamer Tubes

Pad Chambers

Goliath Magnet

Charged Particle Veto-Detector

Target
(inside Plastic-Ball)

Time of Flight (#1)
(PID of negative hadrons)

21.5 m

Start Counter

33 TeV Pb

Multistep Avalanche Chambers
with CCD-readout (tracking of charged particles)

Plastic-Ball
(π^+, p, ... He in target region)

Silicon-Pad and Silicon-Drift Detectors
(pseudorapidity-dist. of charged particles)

interval $3.5 < \eta < 5.5$. The minimum bias trigger required $E_T \gtrsim 5$ GeV and a valid signal from the beam counters. The measured $d\sigma/dE_T$ distribution is used for the calculation of the collision centrality. The minimum bias cross section for the run period used in this analysis is $\sigma_{mb} = 6451$ mb with an overall systematic error of less than 10%.

Two thin circular silicon wafer detectors were positioned at small distance downstream from the target, where charged particle trajectories were not affected by the magnetic field. A silicon pad multiplicity detector, SPMD [16], was located at a downstream distance of 32.85 cm. It was segmented into 184 azimuthal sectors and 22 pseudorapidity rings in the range $2.35 < \eta < 3.75$, and maintained pad occupancy below 20%. The SPMD measured the energy deposited in each pad. A silicon drift detector, SDD [17], was located at a distances of 12.5 cm from the target. Its position resolution was 25 and 35 μm in the azimuthal and radial coordinates, respectively. The acceptance of the two detectors overlapped in the pseudorapidity interval $2.35 < \eta < 3.4$. The two detectors were used for precise reconstruction of the vertex position of the Pb + Pb primary collision. For that purpose straight lines going through each pair of hits in the SDD and SPMD were projected onto the target plane. The one dimensional spatial resolution was found to be better than 0.3 mm perpendicular to the beam line.

The WA98 experiment comprised two charged particle spectrometer arms located on the right (first arm) and the left (second arm, not used in the present analysis) facing downstream from the target, beyond a dipole magnet (Goliath) with 1.6 Tm bending power in the horizontal plane. The first tracking arm consisted of six Multistep Avalanche Chambers, MSAC, read out by CCD cameras equipped with two image intensifiers [18–20]. Each pixel of a CCD viewed a 3.1×3.1 mm^2 area of a chamber. In addition, a 4×1.9 m^2 time-of-flight wall positioned behind

the chambers at a distance of 16.5 m from the target allowed for particle identification with a time resolution better than 120 ps. The TOF detector consisted of 480 scintillator counters with area 3.3×48.5 cm^2 and thickness 2 cm arranged in four rows [21]. Each counter was equipped with two PMTs, one at each end. The position of a hit along a scintillator bar was evaluated using two methods: the first used the time difference of signals obtained from the two ends of the scintillator bar, and the second used the ratio of their amplitudes. Both methods provide a spatial resolution of the order of 2.5 cm.

Tracks were selected which traverse all six MSAC chambers, have detected hits in at least four of them, and were associated with a TOF hit within a 6×6 cm^2 window. An additional momentum dependent time of flight cut was used to exclude misidentified pion, kaon, and proton tracks at a level better than 1%. The $(m_T - m_\pi)$-rapidity acceptance for pions generated by Monte Carlo is shown in Fig. 2.
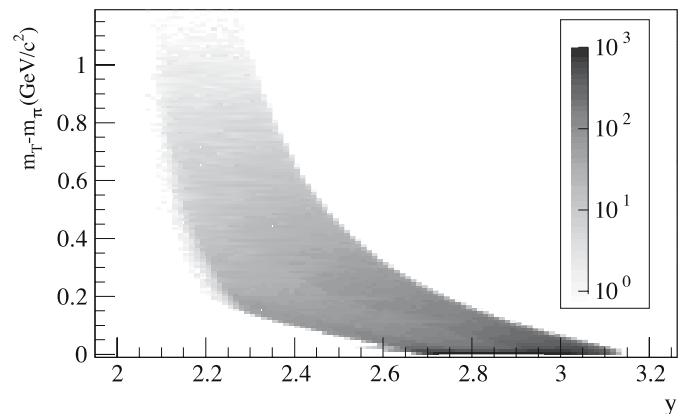

Fig. 2. Acceptance of the first tracking arm in the $(m_T - m_\pi, y)$ plane for pions

The center of mass system rapidity is 2.9. The momentum resolution of the spectrometer was $\Delta p/p = 0.005$ at $p = 1.5\,\mathrm{GeV}/c$.

Positive and negative particles were detected in two sets of runs with opposite direction of the magnetic field. Data samples consisting of $0.58 \times 10^6\,\pi^-$ and $0.22 \times 10^6\,\pi^+$ tracks satisfying all quality requirements were used for the ratio measurement.

Efficiency matrices were measured for a grid of 8×8 cells across each MSAC chamber and for several run periods. The overall tracking arm efficiency measured for negative particles was 2% less than that for positive particles due to chamber instabilities, however, there was no significant difference in the m_T dependence of the efficiencies. The detailed analysis of the π^- and K^- measurement in the first tracking arm has been presented in a separate paper [22].

3 Method of simulation

Simulations have been used in this analysis to estimate the different contributions to the measured R_π and R_K ratios, and to compare with the measured results. A detailed description of the primary collisions, of the Coulomb final state interactions, and of the particle propagation through the experimental setup has been simulated.

The primary Pb + Pb collisions were simulated with the RQMD 2.4 model [13] event generator which reproduces well the light strange baryon yield measured by the WA97 experiment [23], but does not include Coulomb interactions. In RQMD the particles are treated semiclassically over the complete evolution of the system. This allows the calculation of the Coulomb forces between each particle pair as an "afterburner" applied to the RQMD output. The electromagnetic interaction of a particle i with another charged particle j was calculated as described in [24] by

$$m_i \frac{\mathrm{d}u_i^\mu}{\mathrm{d}\tau} = \sum_{j \neq i} \frac{e_i}{c} F_{ij}^{\mu\nu} u_i^\nu \,, \tag{1}$$

where j runs over all charged particles of the system. Here particle i has mass m_i, charge e_i and 4-velocity $u_i = (1, \mathbf{v})/\sqrt{1 - \mathbf{v}^2}$. The tensor $F_{ij}^{\mu\nu}$ is given by

$$F_{ij}^{\mu\nu} = \frac{e_j}{c} \frac{X^\mu u_j^\nu - X^\nu u_j^\mu}{\left(\frac{1}{c^2} \left(u_j^\lambda X^\lambda \right)^2 - X_\lambda X^\lambda \right)^{3/2}} \,, \tag{2}$$

where X^λ is the relative 4-distance between particles i and j. The forces are calculated at each time step of the system evolution and the positions and momenta of the particles are updated with the effect of the Coulomb forces only for those particles which have undergone their last collision. RQMD events with Coulomb interactions added were used as input to the detector simulation. Delta electrons produced by Pb ions in the target material before the collision were also simulated through the detector response.

The GEANT 3.21 program [25] was used for the detector simulation. The target, beam line, Goliath magnet, SDD and SPMD detectors, and tracking arm have been described in detail. For the track reconstruction the same procedure as used in the treatment of real data was employed. For every hit in the tracking arm all information on the particle and all its predecessors was stored for further analysis so that the history of every track could be traced back to the moment of the primary collision.

4 Experimental results

4.1 Centrality selection

The R_π ratio was studied for six centrality intervals defined by the transverse energy E_T measured with the MIRAC. The value of b may be estimated from the measured E_T according to the equation

$$\pi b^2 = \int_{E_\mathrm{T}}^{\infty} (\mathrm{d}\sigma/\mathrm{d}E_\mathrm{T})\,\mathrm{d}E_\mathrm{T} \,, \tag{3}$$

where $\mathrm{d}\sigma/\mathrm{d}E_\mathrm{T}$ is the experimentally measured distribution. Systematic comparisons of $\mathrm{d}\sigma/\mathrm{d}E_\mathrm{T}$ with predictions of VENUS 4.12 [26] and extraction of the number of participating nucleons or number of binary collisions are given in [27]. Table 1 lists the centrality intervals used in this analysis.

4.2 Particle ratios

The two tracking arms of WA98 provide two independent measurements of the pion ratio and have been shown to be consistent [12]. This study focuses on an analysis of the data obtained by the first tracking arm, whose acceptance for pions is shifted by about 0.5 of a unit of rapidity closer to the target fragmentation region relative to the acceptance of the second arm. This provides more favourable conditions for π/K separation in the region of large transverse mass where the normalization of the ratios is performed. At

Table 1. Centrality intervals defined according to the amount of E_T measured in MIRAC. The number of participants was calculated with VENUS 4.12

Centrality interval number	E_T (GeV)	$\sigma/\sigma_\mathrm{mb}$ (%)	Impact parameter (fm)	Number of participants
1	34.5–130	36.8–70.2	8.6–12.0	34–136
2	130–180	28.0–36.8	7.5–8.6	136–179
3	180–240	19.6–28.0	6.3–7.5	179–231
4	240–325	10.1–19.6	4.5–6.3	231–306
5	325–400	3.58–10.1	2.7–4.5	306–364
6	> 400	< 3.58	< 2.7	> 364

low p_T it allows better rejection of electrons through time-of-flight and a significantly larger number of tracks pass through the active area of the SPMD than is the case for the second arm. Figure 3 shows the R_π ratio normalized at transverse kinetic energy between 0.3 and 0.76 GeV/c^2 for the six centrality selections of Table 1. It should be noted that the Coulomb interaction effect on the ratio is strongly reduced and the contribution from hyperon decays is absent in the normalization region.

The e^-/e^+ ratio can be used as a check of the absolute normalization of the R_π ratio. For $0.8 < p < 1.2$ GeV/c electron and positron tracks are well identified through time-of-flight. As imposed by the tracking arm acceptance these tracks have transverse momenta below 50 MeV/c. Since both electrons and positrons originate mainly from photon conversions in the target material their yields should be identical, except for a small additional electron contribution from the production of delta electrons. These purely electromagnetic processes are well understood, so that the ratio e^-/e^+ is expected to be reproduced in simulation with an accuracy of order 1%. The e^-/e^+ ratio is presented in Fig. 4 as a function of centrality and com-

Fig. 4. MIRAC E_T dependence of the e^-/e^+ ratio. The normalization is the same as for the π^-/π^+ ratio. Data are shown by *filled circles*. The *hatched band* indicates the statistical uncertainty (Mean ± RMS) of the RQMD prediction

pared to predictions. For each centrality the e^-/e^+ ratio is normalized with the same normalization used for the corresponding π^-/π^+ ratio in Fig. 3. Any difference between data and simulation is a measure of the systematic error in the normalization of the measured R_π distributions of Fig. 3. Summed over all centrality bins the difference between data and simulation of the e^-/e^+ ratio is $-0.8 \pm 1.2\%$, consistent with the expected accuracy of the comparison. This result indicates that the systematic error on the absolute normalization of R_π introduced by normalization of the ratio in the region $0.3 < m_T - m_\pi < 0.76$ GeV/c^2 is small, and that the normalization error is dominated by the statistical error of the data used for the normalization (shown by the dotted lines in Fig. 3).

The ratio for kaons R_K measured under the same experimental conditions is presented in Fig. 5 for the 10% most central collisions. The kaon ratio shows no signifi-
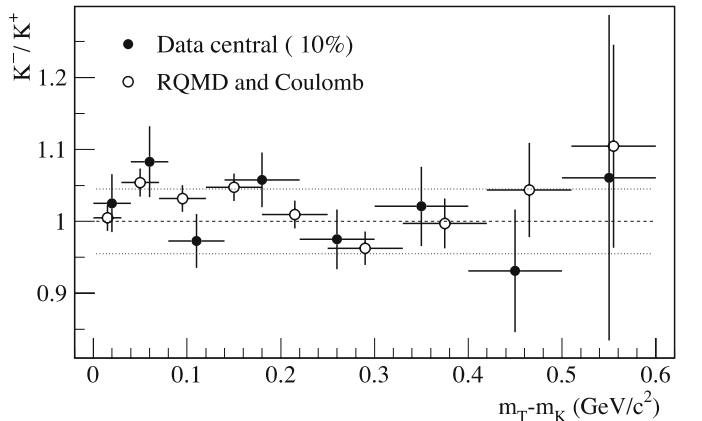

Fig. 3. The ratio R_π vs. $m_T - m_\pi$ for several Pb + Pb collision centrality intervals defined by E_T measured in the MIRAC. Data (*filled circles*) compared with predictions from RQMD including the Coulomb interaction (*open circles*). The ratios are arbitrarily normalized to 1.0 in the region $0.3 < m_T - m_\pi < 0.76$ GeV/c^2. The statistical errors are shown by the *error bars* on the *points*. The *dotted lines* indicate the statistical error on the normalization of the data. The RQMD normalization errors are about half as large

Fig. 5. The kaon ratio for the 10% most central Pb + Pb collisions. Data (*filled circles*) are compared with predictions from the RQMD model with Coulomb interactions included (*open circles*). The ratios are arbitrarily normalized to 1.0 in the region $0.3 < m_T - m_K < 0.6$ GeV/c^2. Errors are as described for Fig. 3

cant dependence on transverse kinetic energy. The lack of enhancement at low transverse mass is consistent with RQMD simulations with Coulomb final state interactions. The acceptance for the lowest transverse mass is located near kaon rapidity $y = 1.8$ in the laboratory system. For $m_T - m_K > 0.2\,\mathrm{GeV}/c^2$ the average rapidity is about $y = 2.15$.

4.3 Hyperon contribution

Pions from hyperon decays have a much steeper transverse momentum spectrum than directly produced pions. Since strange hyperons are more abundantly produced than anti-strange hyperons, the π^-/π^+ ratio will be enhanced at low m_T due to this difference. In order to study the Coulomb effect on the directly produced pions, it is necessary to estimate and remove the hyperon contributions.

The silicon pad multiplicity detector has been used to estimate the yield of identified tracks that do not track back to the target vertex, and thus may be attributed to products of strange or anti-strange hadron decays. All pads of the SPMD that overlap with a $4 \times 4\,\mathrm{mm}^2$ window, centered at the point where the extrapolation of the track towards the target intersects the SPMD plane, were selected. The summed energy loss in the pad window is denoted as S, and given in units of the energy loss of a minimum ionizing particle in the silicon wafer of the SPMD. S therefore gives an estimate of the number of minimum ionizing particles traversing the SPMD within the pad window. Simulation indicates that the mean value over a large set of tracks for pion tracks originating in the target is $\langle S \rangle = 0.89$, while for tracks from hyperon and K_S^0 decays $\langle S \rangle = 0.17$ and 0.20, respectively. This is because tracks that originate from hyperon or K_S^0 decays either traverse the SPMD far from the pad indicated by the extrapolation, or do not traverse it at all (produced downstream of the SPMD). Thus, tracks from hyperon decays will be suppressed by roughly a factor of $0.89/0.17 \approx 5$ with the SPMD hit requirement.

In the case of high pad occupancy the energy loss S_1 measured in the SPMD window associated with the track contains a significant contribution S_2 from spurious tracks. The value of S_2 is estimated by the measured energy loss in a window of the same size centered at a location far from the extrapolated track location (in particular, at a location rotated by $12°$ in azimuth). The RQMD simulation indicates that $\langle S' \rangle = \langle S_1 - S_2 \rangle$ provides a good estimate of $\langle S \rangle$ for each kind of track.

According to RQMD predictions, in the region of transverse kinetic energy above $0.3\,\mathrm{GeV}/c^2$ the contribution of hyperon decays to the pion yield is expected to be below 1%, due to the hyperon decay kinematics. In this region, most of the tracks originate from the target, with less than 8% contribution from K_S decays. Therefore, we may consider these tracks a relatively clean selection of directly produced pions and use them to estimate the quality of the description of the SPMD response in the simulation. As shown in Fig. 6, the extracted number of particles traversing the SPMD $\langle S_1 - S_2 \rangle$ coincides with simulation within errors while the SPMD occupancy varies by more
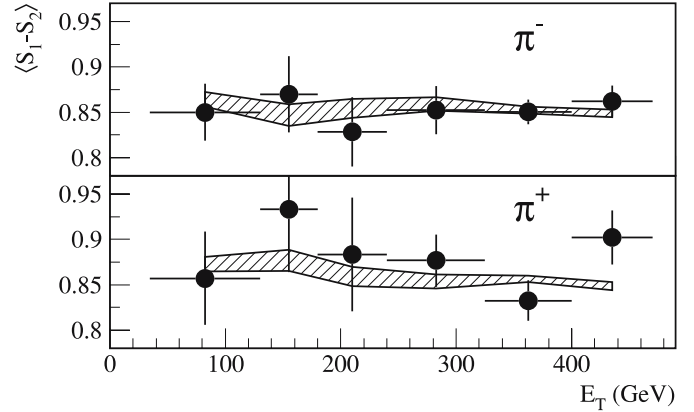

Fig. 6. The corrected average number of minimum ionizing particles, $\langle S' \rangle = \langle S_1 - S_2 \rangle$, as a function of centrality, in the associated SPMD region for negative and positive pions with $m_T - m_\pi > 0.3\,\mathrm{GeV}/c^2$. The results are compared to simulations shown by the *hatched regions*

than a factor of 5 between the most peripheral and most central bins. Mean values of $\langle S_1 - S_2 \rangle = 86.7 \pm 1.4\%$ and $\langle S_1 - S_2 \rangle = 85.4 \pm 0.9\%$ are extracted for positiviely and negatively charged pions, respectively.

For tracks whose extrapolation traverses the SPMD the quantities $R_g = \pi^-/\pi^+$ and $R_{SPMD} = S'^-/S'^+$ are defined, where S'^- and S'^+ are sums of $S_1 - S_2$ values for negative and positive pion tracks identified by the tracking arm. In the case of equal hyperon fractions of the pion yield for both charges one expects $R_{SPMD} \approx R_g$. The behaviour of R_g and R_{SPMD} as a function of transverse kinetic energy for the 10% most central collisions is shown in Fig. 7. Both distributions have the same normalization chosen to give $R_g = 1$ at $m_T - m_\pi > 0.3\,\mathrm{GeV}/c^2$.

Since the contribution to S from hyperon decay tracks is smaller than for tracks originating in the target, a deviation of R_{SPMD} from R_g is an indication of different hyperon fractions in the two charge samples. The observed lower
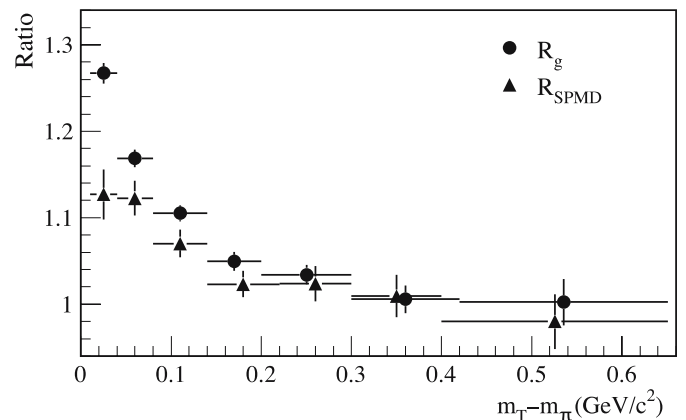

Fig. 7. R_{SPMD} (*triangles*) and R_g (*circles*) for the 10% most central events. See text for definitions of R_{SPMD} and R_g. Both distributions are normalized to 1.0 for R_g at $m_T - m_\pi > 0.3\,\mathrm{GeV}/c^2$

value of R_{SPMD} in comparison to R_{g} for small m_{T} indicates a larger fraction of tracks from hyperon decays in the measured π^- distribution relative to the π^+ distribution. To quantify this difference the quantity $(R_{\mathrm{g}} - R_{\mathrm{SPMD}})/R_{\mathrm{g}}$ is extracted and compared with RQMD simulation as a function of $m_{\mathrm{T}} - m_{\pi}$ in Fig. 8 and as a function of collision centrality in Fig. 9 for $m_{\mathrm{T}} - m_{\pi} < 140\,\mathrm{MeV}/c^2$, where the excess becomes significant. Within errors it is seen that the RQMD simulation provides a good description of the contribution of strange baryon decays to the pion ratio.

The yield distributions of light strange and anti-strange baryons have been reported by the WA97 collaboration [24] and also shown to be successfully reproduced by RQMD calculations. Based on this fact, and on the comparisons of Figs. 8 and 9, the RQMD simulation results have been used to correct the measured pion ratios R_{π} shown in Fig. 3 for the hyperon decay contributions to obtain the corrected ratios R'_{π} of pions originating in the target. For this purpose, for each of the π^- and π^+ yields,

the fraction of the pion yield from strange hadron decays has been estimated from RQMD simulation and removed from the total yield. Figure Fig. 10 shows the corrected pion ratios $R'_{\pi} = \pi^-/\pi^+$.

At low momenta the e^- and e^+ tracks have been separated from pions through time-of-flight and their abundances are found to be in agreement with simulation. At high momenta e^- and e^+ tracks cannot be separated from pions and their relative yields have been estimated from simulation. The ratio R'_{π} of pions originating from the target has also been corrected for e^- and e^+ misidentified as pions at high momenta. According to simulation this e^- and e^+ contamination weakens the enhancement of the pion ratio by about 2% for the lowest m_{T}. The corrected ratios R'_{π} shown in Fig. 10 can be used for comparison of the π^-/π^+ ratio with predictions from models including the decay of the η and other short lived resonances.

In Fig. 11 the dependence of the corrected pion ratio R'_{π} on the collision centrality is shown for two intervals of pion transverse kinetic energy: below $40\,\mathrm{MeV}/c^2$ and between 40 and $140\,\mathrm{MeV}/c^2$. The error due to normalization is included in the error bars. Predictions from RQMD calculations with Coulomb interactions included are also shown. Both the measured results and the RQMD predic-

Fig. 8. $(R_{\mathrm{SPMD}} - R_{\mathrm{g}})/R_{\mathrm{g}}$ for the 10% most central events. Data are shown by *filled circles*. See text for definitions of R_{SPMD} and R_{g}. The *hatched band* indicates the statistical uncertainty (Mean ± RMS) of the RQMD prediction
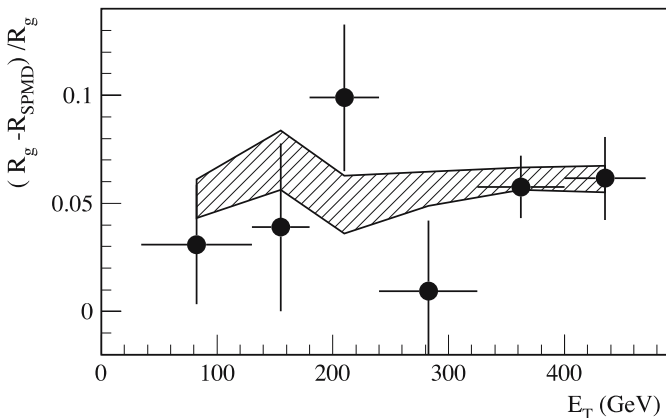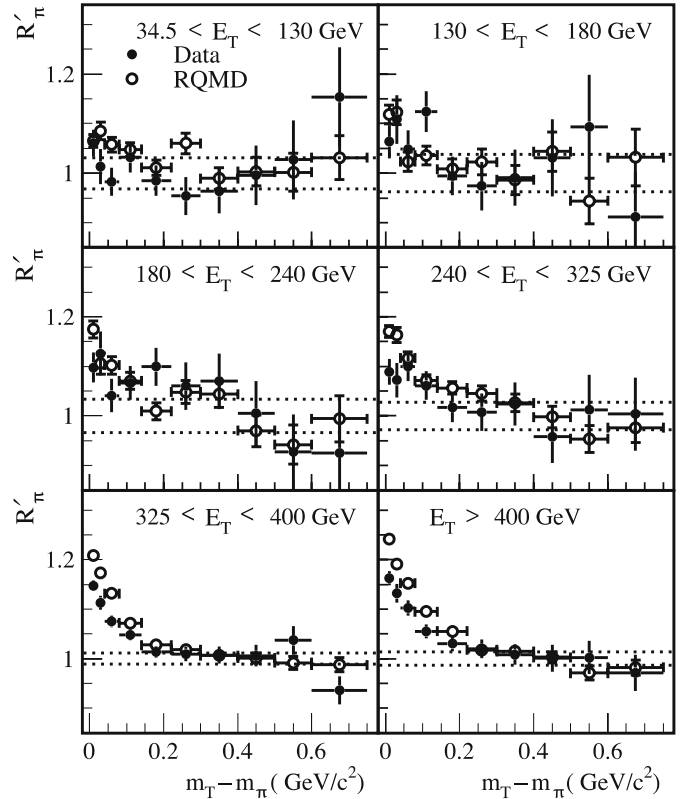

Fig. 9. Centrality dependence of $(R_{\mathrm{SPMD}} - R_{\mathrm{g}})/R_{\mathrm{g}}$ for $m_{\mathrm{T}} - m_{\pi} < 140\,\mathrm{MeV}/c^2$. Data are shown by *filled circles*. The *hatched band* indicates the statistical uncertainty (Mean ± RMS) of the RQMD prediction

Fig. 10. The corrected charged pion ratio $R'_{\pi} = \pi^-/\pi^+$ for pions originating from the target, after removal of the hyperon decay and electron contamination contributions. Data (*filled circles*) are compared with predictions from RQMD including the Coulomb interaction (*open circles*). The ratios are arbitrarily normalized to 1.0 in the region $0.3 < m_{\mathrm{T}} - m_{\pi} < 0.76\,\mathrm{GeV}/c^2$. Errors are as described for Fig. 3
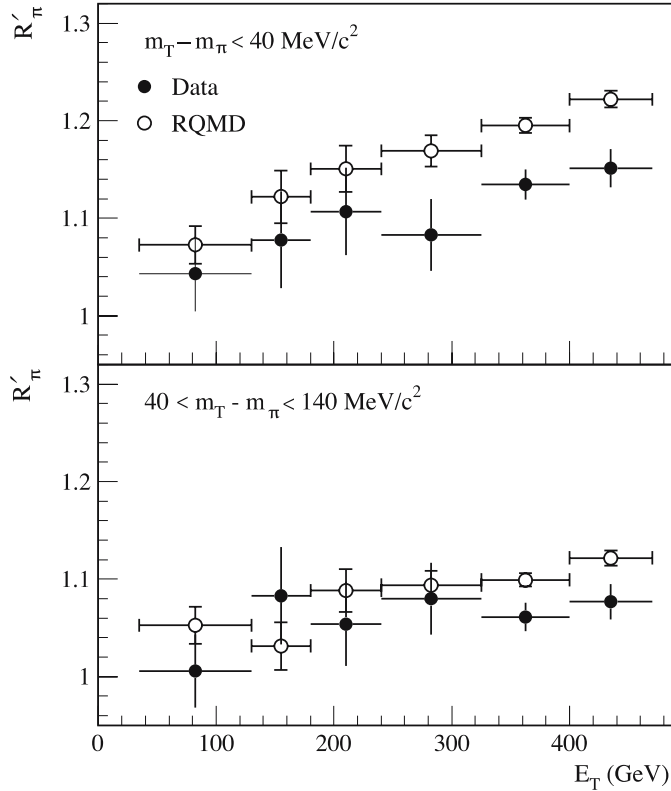
Fig. 11. Centrality dependence of the corrected charged pion ratio for pions originating from the target for $m_T - m_\pi < 40\,\mathrm{MeV}/c^2$ and $40 < m_T - m_\pi < 140\,\mathrm{MeV}/c^2$. Data (*filled circles*) are compared with predictions from RQMD calculations (*open circles*)

tions show a smooth increase of the pion ratio with increasing centrality. As expected, the ratio tends to a value of unity for peripheral collisions. However, RQMD is seen to overpredict the measured pion ratio with a discrepancy that grows with decreasing transverse mass.

5 Modified Coulomb calculations

Several parameters of the collision, such as the total participant charge at central rapidity, its transverse expansion velocity, and the freeze-out time, affect the π^-/π^+ ratio [6]. In order to investigate the sensitivity of the pion ratio to the collision parameters, the Coulomb calculations were repeated under alternative scenarios following minor modifications of the RQMD output. For this study RQMD events from central Pb + Pb collisions with impact parameter $b < 4.5\,\mathrm{fm}$ were used.

In the first modification, the RQMD baryon rapidity density was adjusted. Since the value of dN/dy for protons around mid-rapidity for central Pb + Pb collisions as measured by the NA44 [28] and NA49 [29] experiments is lower than the RQMD prediction by about 30%, the RQMD Coulomb interaction from baryons should be reduced accordingly. The corresponding reduction of the

baryon Coulomb source was implemented in the calculation by weighting the Coulomb charge of all baryons during all stages of the collision by the ratio of measured to predicted proton dN/dy distributions. This baryon rapidity density correction (BRDC) reduces the ratio at the lowest $m_T - m_\pi$ bin by 3% (Fig. 12). Since this correction is based on a discrepancy between RQMD and experimental measurements, further calculations use this modified baryon Coulomb charge rapidity density.

To estimate the sensitivity of the pion ratio to the freeze-out time the application of the Coulomb interaction was simply delayed. The mean time of pion freeze-out at $|y_{CMS}| < 1$ in the central Pb + Pb RQMD events is $15\,\mathrm{fm}/c$. For demonstration, a $2\,\mathrm{fm}/c$ delay was added during which time the particles move freely after freeze-out on their final RQMD trajectories. After propagating freely for $2\,\mathrm{fm}/c$ the pions are then subjected to the Coulomb interactions. At $m_T - m_\pi < 40\,\mathrm{MeV}/c^2$ the resulting ratio shown in Fig. 12 by triangles is reduced with respect to the unmodified RQMD result by 5%. This total reduction of the ratio is similar in magnitude to the difference between the data and the unmodified RQMD simulation results of Fig. 11. Alternatively, increased collective flow in RQMD would result in a larger freeze-out volume and a reduced Coulomb interaction, with a similarly improved agreement with the measurements.

In Fig. 13 the pion ratio measured in this experiment for the 10% most central Pb + Pb collisions is compared with that reported by the NA44 collaboration [5]. Neither RQMD calculations, nor the previously mentioned models [6, 11], predict the observed difference in the two measurements. This could indicate an earlier pion freeze-out in the center of mass rapidity region near $y = 1$ (NA44) relative to that near $y = 0$ (WA98).

The measured K^-/K^+ ratio (Fig. 5) does not show any significant m_T dependence. This is consistent with the data of the NA44 collaboration and with RQMD predictions. The kaon ratio enhancement induced through the
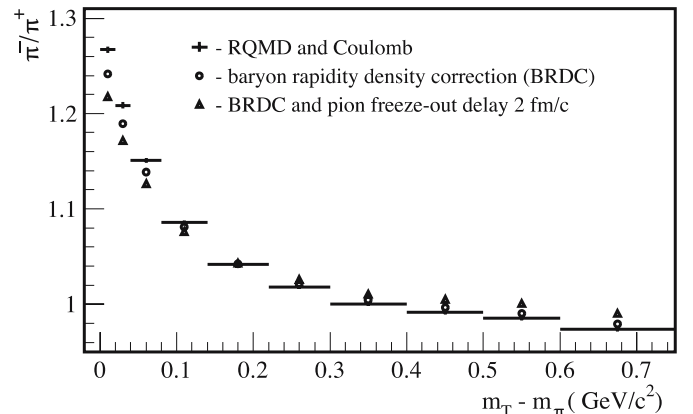

Fig. 12. The pion yield ratio π^-/π^+ at mid-rapidity ($1 < |y_{CMS}|$). Predictions from RQMD with final state Coulomb interaction unmodified (*crosses*), with BRDC (*circles*), and with BRDC and pion freeze-out delayed an additional $2\,\mathrm{fm}/c$ (*triangles*)
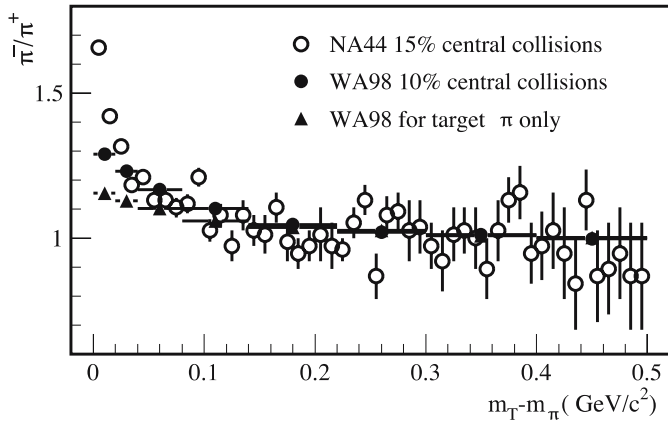
Fig. 13. Comparison of NA44 data (*open circles*) and WA98 data (*filled circles*) for the 10% most central collisions. The ratio for pions originating in the target is also shown (*triangles*)

Coulomb interaction is expected to be less than that for pions by a factor equal to their mass ratio m_π/m_K [7]. However, according to RQMD predictions without Coulomb correction, the kaon ratio has a $\sim 6\%$ drop at low transverse kinetic energy as a result of the greater amount of absorption of K^- than K^+. This large absorption effect must be taken into account when investigating Coulomb effects in the analysis of the kaon ratio data.

6 Discussion and conclusions

The π^-/π^+ ratio has been measured as a function of transverse mass and centrality in Pb + Pb collisions at $158\,A\mathrm{GeV}/c$. The hyperon decay contribution has been deduced and shown to result in an increase of the pion ratio at low m_T that is responsible for about half of the enhancement of π^- relative to π^+ in central collisions, and an even larger fraction of the enhancement in peripheral collisions. The RQMD model was shown to agree with the measured hyperon decay contributions. The hyperon decay contributions have been removed from the measured ratios to extract the ratios for directly emitted pions.

The low m_T enhancement of the π^-/π^+ ratio, after removal of the hyperon decay contribution, increases with collision centrality and tends to zero for the most peripheral events (see Fig. 10). This observation is consistent with the hypothesis that the enhancement is due to the Coulomb interaction induced by the net positive charge of the participant protons. The same behaviour is observed in the framework of RQMD model simulations that include final state Coulomb interactions. However, the RQMD simulation overpredicts the observed enhancement in the ratio by a factor of about 1.5.

Investigations of the RQMD model predictions suggest that rather small modifications of the properties of the participant fireball are necessary to obtain good agreement with the data. For example, good agreement can be achieved after reduction of the baryon rapidity charge density predicted by RQMD according to the NA44 and NA49 proton measurements, together with a small increase of the mean pion freeze-out time (such as an increase from an average of 15 fm/c to 17 fm/c). According to RQMD predictions, the transverse flow velocities of heavy particles are less than those of pions [30]. A slight increase of the baryon transverse flow velocity would have a similar effect as the delay of the freeze-out time. In both cases, the system disperses over a larger volume before freeze-out, which reduces the Coulomb field and, therefore, the π^-/π^+ ratio. Based on comparisons with the RQMD model calculations, the results suggest a relatively large value of the mean freeze-out time for pions (~ 15 fm/c) in central Pb + Pb collisions.

References

1. D. Pelte et al., Z. Phys. A **357**, 215 (1997)
2. L. Ahle et al., Nucl. Phys. A **610**, 139 (1996)
3. L. Ahle et al., Phys. Rev. C **57**, R466 (1998)
4. C. Müntz, Acta. Phys. Polon. B **29**, 3253 (1998)
5. H. Bøggild et al., Phys. Lett. B **372**, 343 (1996)
6. H.W. Barz et al., Phys. Rev. C **56**, 1553 (1997)
7. H.W. Barz et al., Phys. Rev. C **57**, 2536 (1998)
8. H. Heiselberg, Nucl. Phys. A **638**, 479 (1998)
9. A. Ayala et al., Phys. Rev. C **59**, 3324 (1999)
10. T. Osada et al., Phys. Rev. C **55**, 2615 (1997)
11. T. Osada, Y. Hama, Phys. Rev. C **60**, 034904 (1999)
12. F. Retiere et al., Nucl. Phys. A **681**, 149 (2001)
13. H. Sorge, Phys. Rev. C **52**, 3291 (1995)
14. WA98 Collaboration, Preprint CERN/SPSLC 91-17, SPSLC/P260 (1991)
15. T.C. Awes et al., Nucl. Instrum. Methods A **279**, 479 (1989)
16. W.T. Lin et al., Nucl. Instrum. Methods A **389**, 415 (1997)
17. E. Gatti, P. Rehak, Nucl. Instrum. Methods A **225**, 608 (1984)
18. J.M. Rubio et al., Nucl. Instrum. Methods A **367**, 358 (1995)
19. A.L.S. Angelis et al., Nucl. Phys. A **566**, 605 (1994)
20. M. Iżycki et al., Nucl. Instrum. Methods A **310**, 98 (1991)

21. V.V. Avdeichikov et al., JINR **8**, 23c (1997)
22. M.M. Aggarwal et al., Phys. Rev. C **67**, 014 906 (2003)
23. F. Antinori et al., Eur. Phys. J. C **11**, 79 (1999)
24. F. Gastineau, J. Aichelin., Phys. Rev. C **65**, 014 901 (2002)
25. R. Brun et al., GEANT3, CERN/DD/cc/84-1

26. K. Werner, Phys. Rep. **232**, 87 (1993)
27. M.M. Aggarwal et al., Eur. Phys. J. C **18**, 651 (2001)
28. I.G. Bearden et al., Phys. Lett. B **388**, 431 (1996)
29. S.V. Afanasiev et al., Nucl. Phys. A **160**, 76 (1996)
30. H. Sorge, Phys. Lett. B **373**, 16 (1996)